

Dynamic Adsorption Model Fitting Studies of Typical VOCs Using Commercial Activated Carbon in a Fixed Bed

Dongdong Zhang · Jin Cao · Guiping Wu · Longzhe Cui

Received: 13 December 2017 / Accepted: 21 February 2018 / Published online: 22 May 2018
© Springer International Publishing AG, part of Springer Nature 2018

Abstract The adsorption behaviors of five typical volatile organic compounds (VOCs) onto one commercial activated carbon (CAC) in a fixed bed were investigated in this study. The selected CAC as a model adsorbent has a high surface area of $1099.74 \text{ m}^2 \text{ g}^{-1}$. Moreover, five kinds of typical VOCs, including acetone, ethyl acetate, propyl acetate, butyl acetate, and isopropanol, were chosen as the target pollutants. The adsorption capacities of the above VOCs were 289.8, 389.4, 443.7, 467.4, and 474.3 mg g^{-1} , respectively. The adsorption data were fitted by using two dynamic adsorption models (Boltzmann and Yoon-Nelson) and four kinetic models (pseudo-first-order, pseudo-second-order, Elovich and Banham adsorption rate equation). Compared to other models, the Boltzmann model and the Banham adsorption rate equation could well fit the data of the selected sorption periods. These observations indicated that the fixed bed has a small effect of the mass transfer resistance and a high utilization for the

adsorbent. Meanwhile, the Banham adsorption rate equation also could well predict the real condition and the maximum adsorption capacity of the adsorbent. Therefore, the present study clarified the adsorption dynamic behaviors of the selected VOCs onto the CAC in a fixed bed. We believe that the finding of this work is helpful to optimize the design of dynamic adsorption system for the removal of VOCs.

Keywords VOCs · Activated carbon · Dynamic modeling · Fixed bed system · Mechanism study

1 Introduction

In the last decades, air pollution has become one of the most stringent environmental challenges. As one of the main air pollutants, volatile organic compounds (VOCs) can be generated from various ways, such as chemical, petrochemical, pharmaceutical, motor vehicles, and construction industry (Celebioglu et al. 2016). According to the definition given by the World Health Organization (WHO), VOCs are organic compounds with boiling points ranging from 50–100 to 240–260 °C (Stolwijk 1990). Because of their high vapor pressure, VOCs can easily evaporate into the atmosphere. For this, VOCs are regarded to be one of the major contributors to the formation of photochemical smog and secondary organic aerosols (SOA), which may cause short- or long-term adverse health risks for humans even at very low concentrations (Volkamer et al. 2006). Thus, it is very important to develop effective methods for

Highlights · A new type of adsorption device was used for VOC adsorption.

- Dynamic adsorption behaviors of VOCs onto CAC in a fixed bed were investigated.
- Various dynamic and kinetic models were fitted to five typical VOC.
- Boltzmann model could better describe the dynamic adsorption behavior.
- Banham adsorption rate equation evaluated the maximum uptake more accurately.

D. Zhang · J. Cao · G. Wu · L. Cui (✉)
College of Resources and Environmental Science, South-Central University for Nationalities, Wuhan, Hubei 430074, China
e-mail: cuilonger@hotmail.com

controlling VOC emission into the natural environment. In this perspective, diverse technologies have been developed for removal of VOCs, including adsorption (Chiang et al. 2002; Gil et al. 2014), absorption (Dumont et al. 2011), condensation (López-Fonseca et al. 2004), catalytic oxidation (Qian et al. 2016), and microbial degradation (Guieysse et al. 2008). Among the above techniques, adsorption has been widely recognized as a more cost-effective and eco-friendly method for VOC abatement, especially at low concentration. One of the key points by applying adsorption technology is to find a high-performance adsorbent. So far, various natural or synthetic adsorbents with amorphous or microcrystalline structure, including activated carbon, zeolites, alumina, silica gel, and synthetic polymers, have been studied for the removal of VOCs (Xijun et al. 2001; Das et al. 2004; Zaitan et al. 2016; He et al. 2017).

Among the above adsorbents, activated carbon (AC) is one of the most common one for VOC removal, mainly due to its highly developed surface area, large pore volumes, thermos stability, and benign sorption capacities (Aygün et al. 2003). In general, the adsorption method of VOCs on AC contains static and dynamic approaches. Comparing to the former technique, dynamic adsorption method is used more extensively, owing to its less time consumption but higher removal efficiency (Huang et al. 2002). Fixed bed systems packed with ACs are normally employed for the dynamic removal of VOCs from the gas phase (Mohan et al. 2009; Giraudet et al. 2014; Guo et al. 2014; Tefera et al. 2014). The general adsorption process of VOCs in the fixed bed by ACs is as follows: (a) mass transfer of the substance from the gas phase to the surface of the adsorbent (convection, axial dispersion, diffusion of particles through the film); (b) mass transfer of the adsorbent in the pore structure (pore diffusion); and (c) adsorption/desorption on the surface pores of the adsorbent (surface reaction). When the equilibrium state is achieved, the breakthrough times can be measured based on the remaining VOCs around their 10% initial concentrations.

Although related studies have reported the removal of VOCs by using ACs, most of them so far focused on the macroscopic adsorption efficiencies of ACs, including sorption rates and maximum uptakes (Chuang et al. 2003; Ebner et al. 2006; Biesheuvel et al. 2009). In other words, few researches studied the dynamic adsorption behaviors of VOCs onto ACs in detail. Therefore, in this

work, we aim to investigate the dynamic adsorption behaviors of five typical VOCs onto one CAC in a fixed bed system through model fitting. The theoretical Boltzmann and Yoon-Nelson models were used to simulate the experimental data to predict the breakthrough behaviors of the selected VOCs. Moreover, four types of kinetic models (pseudo-first-order, pseudo-second-order, Elovich kinetic equation, and Banham adsorption rate equation) were introduced in order to further clarify the dynamic sorption process.

2 Materials and Methods

2.1 Materials

Five analytical grade VOCs (acetone, propyl acetate, butyl acetate, ethyl acetate, and isopropyl alcohol) are purchased from Sinopharm Group Chemical (China). The anthracite coal base of activated carbon was purchased from Ningxia Huahui Activated Carbon Company. The granular activated carbon was selected from 1 to 1.5 mm in diameter. All chemicals were used without further purification. The physical/chemical properties of the VOCs are listed in Table 1.

2.2 Experimental Setup and Procedure

As shown in Fig. 1, the setup consists of two mainly functional sections for the preparation of gas-VOC vapor mixture and the adsorption process in the fixed bed.

In the former section, VOC solution in the gas generator (1), nitrogen (Wuhan City Xiangyun Industry and Trade Limited Liability Company, China) with a purity of 99.999%, was used as the carrier gas. The flow rate of gas stream was controlled by a valve (3) and measured by a flow meter (2). The initial concentrations of five volatile organic compounds were controlled at 500 mg/m³. The combination of infrared carbon fiber heating and quartz spiral tubes (4) was used for heating adsorption. In addition, it also can be used for desorption process. The air temperature inside the enclosure was measured by a digital thermometer (5). The part of fixed bed mainly has an adsorption column (7) and a digital balance (11). The glass column was packed with around 100 g of the AC. The gas mixture was fed into the bottom of the column, and up-flowed through the adsorbent fixed bed (inner diameter 5.2 cm, height 28 cm)

Table 1 Physico-chemical properties of five kinds of VOCs

| VOCs species | Molecular formula | Kinetic diameter (nm) | Formula weight (g mol ⁻¹) | Ionization potential (eV) | Boiling point (°C) |
|-------------------------|--|-----------------------|---------------------------------------|---------------------------|--------------------|
| Acetone (CP) | CH ₃ COCH ₃ | 0.46 | 58.08 | 9.71 | 56.53 |
| Isopropyl alcohol (IPA) | (CH ₃) ₂ CHOH | 0.58 | 60.06 | 10.12 | 82.45 |
| Ethyl acetate (EAC) | CH ₃ COOC ₂ H ₅ | 0.84 | 88.11 | 10.01 | 77.20 |
| Propyl acetate (NPAC) | CH ₃ COOCH ₂ CH ₂ CH ₃ | 1.10 | 102.13 | 10.04 | 101.60 |
| Butyl acetate (BAC) | CH ₃ COO(CH ₂) ₃ CH ₃ | 1.20 | 116.16 | 10.00 | 126.50 |

Note: Kinetic diameter reference. CP (Gales et al. 2000); IPA (Fuertes and Centeno 1998); EAC (Gales et al. 2000); NPAC (Huang and Sundmacher 2007); BAC (Fujita et al. 1960)

until the bed was saturated. The temperature of the gas in the column was measured by a digital thermometer (6). The digital balance (11) was used to measure the amount of the adsorbed VOCs based on the increase of the column weight. These data were output by a computer. The outlet concentrations of VOCs were measured by a VOC analyzer (PGM-7300, RAE Systems) (8). The equipment was fitted in an enclosure with a Teflon tube (14), which was used for the insulation.

2.3 Characterization of the CAC

The measurements of surface area and pore size were carried out by N₂ adsorption–desorption isotherms at 77 K using a surface area analyzer (QuantaChorm AUTOSORB-iQ MP). The BET surface area (S_{BET}) was calculated by Quantachorm™ ASiQ software using the Brunauer–Emmett–Teller (BET) equation in a relative pressure range of $P/P_0 = 0.05–0.125$. Total porous

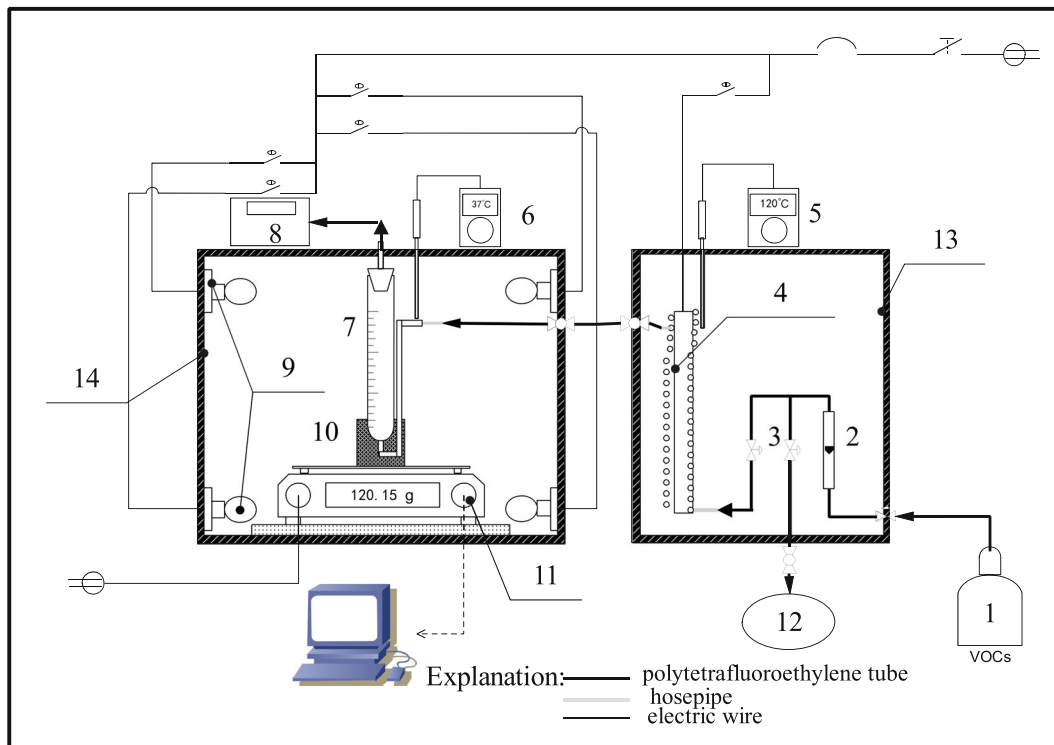


Fig. 1 Experimental setup of the fixed bed for VOC adsorption using the CAC (1, gas generator; 2, flow meter; 3, valve; 4 quartz spiral tube combination; 5 and 6, digital thermometer; 7,

adsorption column; 8, VOC analyzer; 9 and 10, plastic support block; 11, digital balance; 12, waste bag; 13 and 14, Teflon tube).

volume (V_T) was measured at $P/P_0 = 0.995$ (Basta et al. 2009), the micropore volume (V_μ) was determined using the t-plot method (Hudec et al. 2002), and the mesopore volume (V_M) was calculated by the difference between the total pore volume and the micropore volume ($V_T - V_\mu$). The average pore diameter (d_p) was obtained using the ratio $4V_T/S_{BET}$, and pore size distribution was calculated according to the Density Functional Theory (DFT) (Landers et al. 2013). Raman spectra were obtained with a Thermo Fisher DXR spectrometer using a 532 nm Ar line as an excitation source and an acquisition rate of 62 scans s^{-1} between 0 and 4000 cm^{-1} at a 0.5 cm^{-1} interval.

2.4 Dynamic Adsorption of Models

The dynamic adsorption/desorption experiments of the selected VOCs were investigated with a flow rate of 0.02 m/s. To better understand the adsorption processes of the VOCs in the fixed bed, two dynamic adsorption models (Boltzmann and Yoon-Nelson) and four kinetic models (pseudo-first-order, pseudo-second-order, Elovich and Banham adsorption rate equation) were investigated. The equation and parameters of these models were listed in Table 2.

$1/dx$ is the slope at the half concentration ($C/C_0 = 0.5$) point of the penetration curve; A_1 and A_2 separately are the starting and ending points of the curve; x_0 is the time of the half concentration point; t is the penetration time, τ is the time of the half breakthrough point; K' is the

Table 2 Equations and parameters of dynamic adsorption and kinetic model

| | | |
|--------------------|---------------------------------|---|
| Dynamic adsorption | Boltzmann | $y = \frac{A_1 - A_2}{1 + e^{(x-x_0)/dx}} + A_2$ |
| | Yoon-Nelson | $t = \tau + \frac{1}{K'} \ln\left(\frac{1}{K'}\right)$ |
| Kinetic | Pseudo-first-order | $q_t = q_c[1 - \exp(-k_1 t)]$ |
| | Pseudo-second-order | $q_t = \frac{k_2 q_c^2 t}{1 + k_2 q_c t}$ |
| | Elovich | $q_t = \frac{1}{\beta_E} \ln \frac{1}{\beta_E} + \frac{1}{\beta_E} \ln t$ |
| | Banham adsorption rate equation | $q_t = q_c[1 - \exp(-k t^z)]$ |

adsorption rate constant; C and C_0 are the inlet and outlet concentrations of the VOC gas, respectively; k_1 and k_2 are the adsorption rate constants of pseudo-first-order and pseudo-second-order models, respectively; a_E is initial adsorption rate constant and β_E is desorption rate constant; z is a constant; k is a constant (min^{-z}).

3 Results and Discussion

3.1 Characteristics of the CAC

As shown in Fig. 2, the N_2 adsorption/desorption isotherms of the CAC could be identified as type I according to the IUPAC classification. A remarkable uptake at

Fig. 2 Nitrogen adsorption–desorption isotherms of the CAC

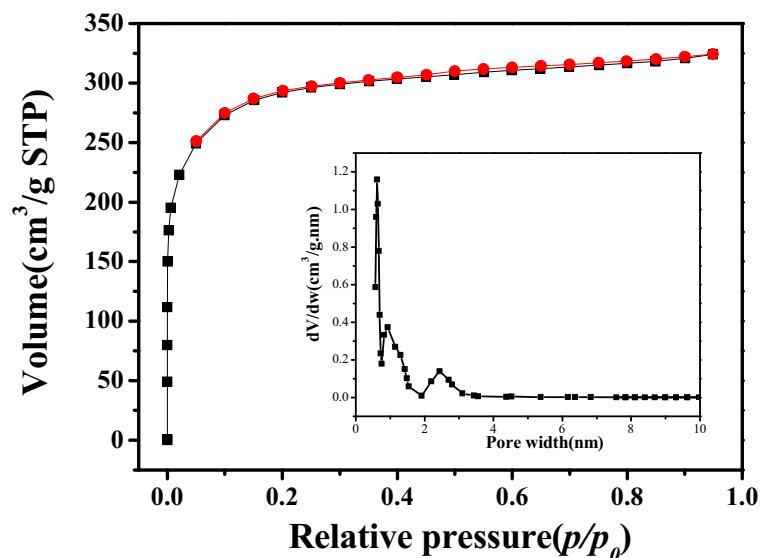
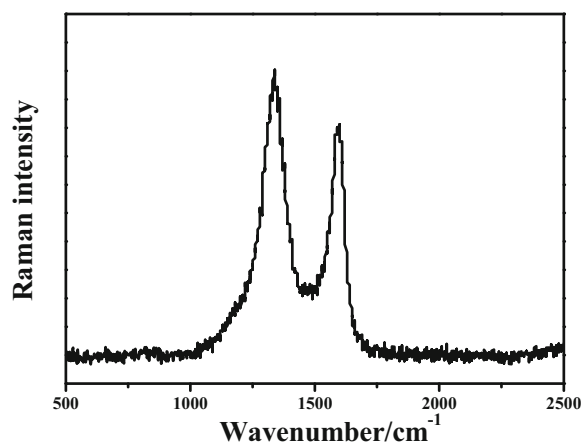


Table 3 Textural properties of active carbon

| Adsorbent | S_{BET} ($\text{m}^2 \text{g}^{-1}$) | S_{micro} ($\text{m}^2 \text{g}^{-1}$) | V_g ($\text{m}^3 \text{g}^{-1}$) | $V_{g_{\text{micro}}}$ ($\text{m}^3 \text{g}^{-1}$) | D_{pore} (nm) |
|---------------|---|---|--------------------------------------|---|------------------------|
| Active carbon | 1099.743 | 1005.954 | 0.461 | 0.415 | 0.614 |

a relative low pressure (P/P_0) was found, indicating abundant micropores of the CAC. Meanwhile, a narrow hysteresis loop started at a P/P_0 ratio of 0.45, which illustrated that the CAC also contains a little mesoporous. Textural characteristics of the CAC are listed in Table 3. The specific and micropore surface areas of the CAC are 1099.734 and 1005.954 m^2/g , respectively. The percentage of micropores is 90.02%. Based on the above findings, the selected CAC is rich in micropores, which is beneficial for the adsorption of the VOCs (Franz et al. 2000).

The result of the Raman spectrum for the CAC is shown in Fig. 3. The peaks at 1340 and 1600 Raman shift (cm^{-1}) belonging to the so-called D band and G band can be separately recognized as the disordered structure carbon and graphitic carbon (Guo et al. 2014). The relative intensities (R) of the D-band and G-band (I_D/I_G) are used to evaluate the graphitic degree in the amorphous carbon. The I_D/I_G ratio of the active carbon sample is 1.24. It indicates that the CAC has a certain lattice oxygen defects and graphite chemical microcrystalline structure, which can enhance the adsorption capacity of the CAC.

**Fig. 3** The Raman spectrum of the CAC

3.2 Dynamic Adsorption and Desorption Performance Studies

In the adsorption/desorption process, the inlet flow rate of the VOCs was fixed to be 0.021 m/s, and the N_2 rate used for desorption was 10 L/min at 25 °C. From Fig. 4 (black curves), the dynamic adsorption process can be divided into three stages: adsorption saturation area, adsorption mass transfer area, and adsorption bed unsaturated adsorption area. At the beginning of the adsorption process, VOC adsorption took place mainly at the lower end of the activated carbon column, and the outlet gas concentration was about 0. As the adsorption proceeds, the mass transfer zone moves up gradually. When the mass transfer zone arrived at the top of activated carbon column, the penetration phenomenon occurred and the concentration of outlet gas gradually increased. After activated carbon in column was saturated, which means that the concentration of the outlet was approximately equal to that of inlet, the adsorption was completed and desorption would be started. Moreover, Table 4 listed the related values of the parameters. The saturated adsorption capacities (q_s) of the five VOCs (acetone, ethyl acetate, propyl acetate, butyl acetate, and isopropanol) were 289.8, 389.4, 443.7, 467.4, and 474.3 mg g^{-1} , respectively. The breakthrough times (t_b) of these VOCs were 3, 36, 78, 54, and 202 min, respectively. The results show that adsorption capacities increased in the order of acetone, isopropanol, ethyl acetate, propyl acetate, and butyl acetate, due to the adsorption of five kinds of VOCs on activated carbon, which is consistent with the variation of molecular weight of adsorbates and the boiling point. The adsorption capacity is usually proportional to the relative molecular mass of the adsorbate; the greater the molecular weight, the better the adsorption performance (Wood 2002), the larger the relative molecular weight of VOCs, the greater the polarity, the easier to be adsorbed by the polar groups on the surface of the activated carbon. In addition, the higher the boiling point of the adsorbate, the lower the saturated vapor pressure, the greater the

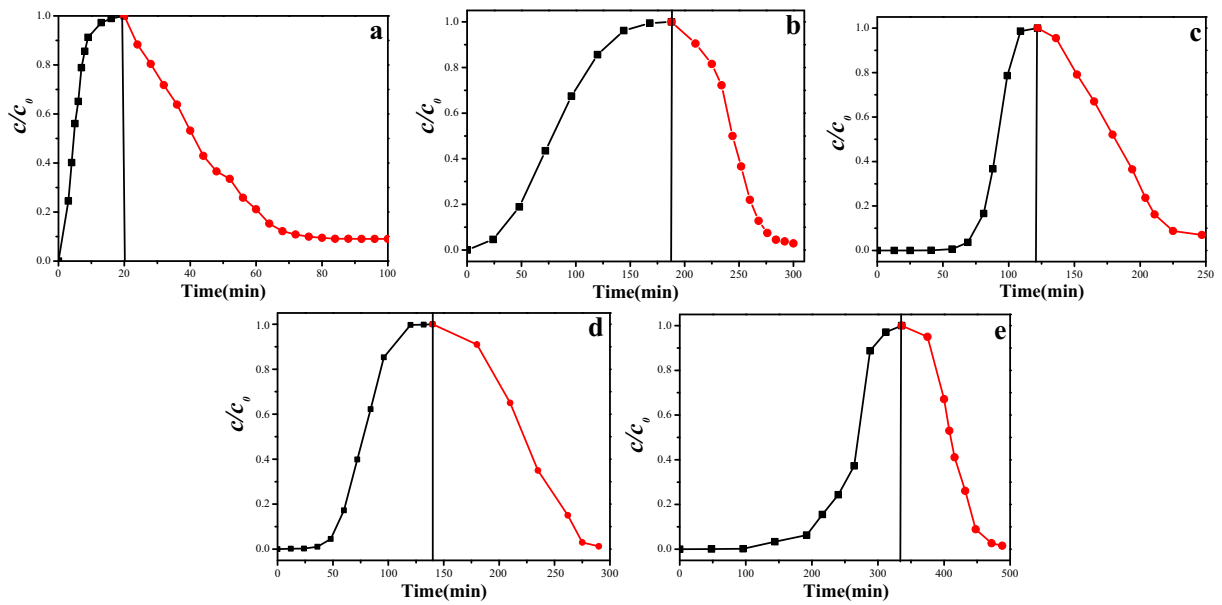


Fig. 4 Adsorption–desorption curves of the VOCs: (a) acetone, (b) isopropyl alcohol, (c) ethyl acetate, (d) propyl acetate, and (e) butyl acetate

equivalent force between molecules, resulting in increased adsorption capacity.

For the desorption processes (red curves shown in Fig. 4), the desorption times of the above VOCs were 80, 112, 135, 150, and 152 min, respectively. Moreover, the desorption efficiencies of the VOCs were ranging from 91 and 99%. These indicated that the CAC has a good reuse potential for the removal of the VOCs. Furthermore, the high desorption efficiencies were

achieved just with the increase of the desorption temperatures. It thus demonstrated that the adsorption of the VOCs by the CAC was supposed to be reversible processes. In other words, the physisorption is more plausible to illustrate the sorption process of the VOCs in the present study. The dominant binding force involved in the sorption mechanism is suggested to be the Van der Waals force between the VOC molecules and the micropores of the CAC (Shroder et al. 1990).

Table 4 Dynamic adsorption experiments data of VOCs on fixed bed. The breakthrough time (t_b) and saturation time (t_s) are defined as the time when $C/C_0 = 10\%$ (C is the outlet gas concentration and C_0 the inlet gas concentration) and C/C_0 reaches about 100%, respectively. The VOC quantum absorbed onto the AC before t_b

and t_s are recorded as breakthrough adsorption capacity and saturated adsorption capacity. Desorption time (t_d) means the time that VOCs adsorbed by activated carbon removed during temperature desorption process, and the desorption rate is the ratio of the mass of the heated desorbed VOCs to the mass of adsorbed VOCs

| VOCs species | Breakthrough process | | Saturation process | | Desorption process | |
|-------------------|--------------------------------|---|-----------------------------|---|-----------------------------|----------------------|
| | Breakthrough point t_b (min) | Breakthrough adsorption capacity q_b (mg/g) | Saturation time t_s (min) | Saturation adsorption capacity q_s (mg/g) | Desorption time t_d (min) | Desorption ratio (%) |
| Acetone | 3 | 5.98 | 28 | 289.8 | 80 | 91.96 |
| Isopropyl alcohol | 36 | 12.43 | 188 | 389.4 | 112 | 95.97 |
| Ethyl acetate | 78 | 32.18 | 122 | 443.7 | 135 | 94.02 |
| Propyl acetate | 54 | 24.69 | 140 | 467.4 | 150 | 98.74 |
| Butyl acetate | 202 | 19.4 | 336 | 474.3 | 152 | 98.48 |

Table 5 Estimated parameters of the Boltzmann and Yoon-Nelson models for the VOCs (mass transfer coefficient ($1/dx$), adsorption rate constant (K'), half breakthrough time (τ), and correlation coefficient (R^2))

| VOC species | Boltzmann | | Yoon-Nelson | | | |
|-------------------|-----------|-------|-------------------|-------------------|-------|----------------------|
| | $1/dx$ | R^2 | τ/min | | R^2 | K'/min^{-1} |
| | | | Fitting data | Experimental data | | |
| Acetone | 0.5566 | 0.999 | 5.114 | 5 | 0.966 | 0.529 |
| Isopropyl alcohol | 0.0426 | 0.997 | 85.705 | 80 | 0.988 | 0.114 |
| Ethyl acetate | 0.1684 | 0.999 | 92.343 | 90 | 0.987 | 0.042 |
| Propyl acetate | 0.0893 | 0.999 | 86.812 | 78 | 0.975 | 0.058 |
| Butyl acetate | 0.0661 | 0.999 | 274.936 | 270 | 0.957 | 0.194 |

3.3 Dynamic Model Fitting Studies of the Breakthrough Curves

In general, the dynamic adsorption process in the fixed bed can be divided into three stages: adsorption saturation area, adsorption mass transfer area, and unsaturated adsorption area of the fixed bed (Dobre et al. 2014). Additionally, the parameter of $1/dx$ (shown in Table 5) means that the higher of the value, the less the mass transfer resistance. Thus, the shorter mass transfer zone normally leads to the higher utilization efficiency of the adsorbent in the fixed bed system (Price and Schmidt 1998). As can be seen from Fig. 5, the breakthrough curves of all the VOCs belong to the typical S shape. In addition, from Table 5, the high correlation coefficient (R^2) values (above 0.99) indicate good fittings by using Boltzmann model. Comparing to the other four VOCs (shown in Fig. 5), the S-shaped part of the breakthrough

curve assigning to acetone is closed to a straight line, indicating the smallest mass transfer resistance and the highest bed utilization efficiency for the adsorption of acetone. The highest mass transfer coefficient value (0.5566) of acetone shown in Table 5 further confirmed the above findings.

The linear Yoon-Nelson model is another approach to describe the adsorption behaviors of the VOCs. As shown in Fig. 6, the linear model could also well fit the experimental data. It was further confirmed based on the high correlation coefficient R^2 values of greater than 0.95 (shown in Table 5). The predicted half breakthrough times (τ) by the linear model were closed to the experimental data. Thus, the predicted parameter values are beneficial for the design of the practical engineering application. In addition, from Table 5, the values of adsorption rate constant (K') decreased with the increase in the molecular diameters of the VOCs. It

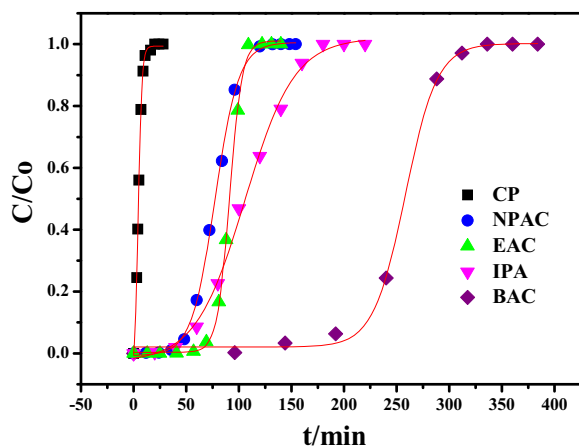


Fig. 5 Boltzmann model fitting of breakthrough curves for the VOCs

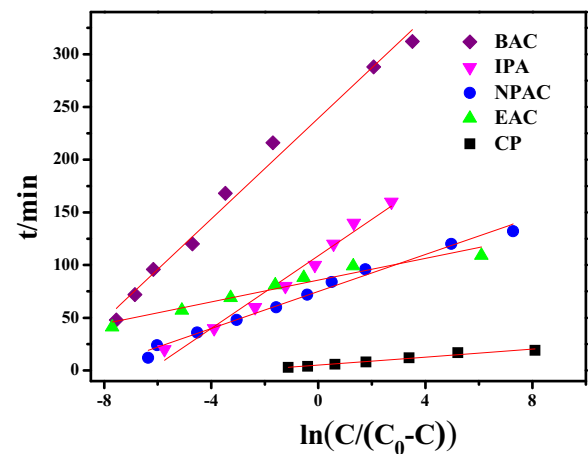


Fig. 6 Yoon-Nelson model fitting of breakthrough curves for the VOCs

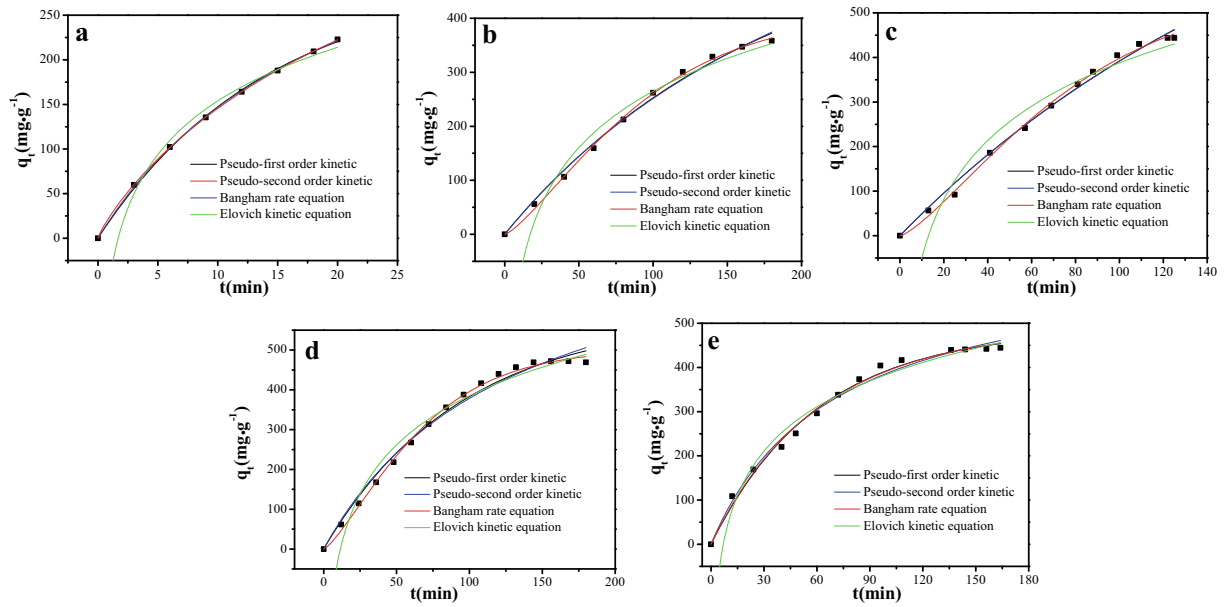


Fig. 7 Non-linear fits of pseudo-first-order kinetic model, pseudo-second-order kinetic model, Banham adsorption rate equation, and Elovich kinetic equation: (a) acetone, (b) isopropyl alcohol, (c) ethyl acetate, (d) propyl acetate, and (e) butyl acetate

can be explained as follows: the pore wall superimposed force is enhanced with the increase of the adsorbate molecule diameter. Owing to the above interference force, the diffusion effect of the adsorption process is

significantly increased, which may decrease the adsorption rates of the VOCs. To further explore the adsorption process, four kinetics model fitting studies were investigated in the following section.

Table 6 Estimated parameters of the four kinetic models (maximum adsorption capacity (q_e), kinetics parameters (K), correlation coefficient (R^2), normalized standard deviations (Δq_e), initial adsorption rate constant (α_E), and desorption rate constant (β_E))

| | | Acetone | Isopropyl alcohol | Ethyl acetate | Propyl acetate | Butyl acetate |
|-----------------------------------|--|------------------------|------------------------|------------------------|------------------------|------------------------|
| $q_{e,exp}$ (mg g ⁻¹) | | 289.8 | 389.4 | 443.7 | 467.4 | 474.3 |
| Pseudo-first-order kinetic model | q_e (mg g ⁻¹) | 291.2389 | 575.7781 | 958.0862 | 582.7614 | 485.5442 |
| | k_1 (min ⁻¹) | 0.0706 | 0.0058 | 0.0526 | 0.0107 | 0.01664 |
| | R^2 | 0.999 | 0.994 | 0.993 | 0.991 | 0.993 |
| | Δq_e (%) | 0.49 | 32.37 | 53.69 | 19.80 | 2.32 |
| Pseudo-second-order kinetic model | q_e (mg g ⁻¹) | 447.2629 | 964.3208 | 1708.2934 | 871.7189 | 656.6106 |
| | k_2 (min ⁻¹) | 1.094×10^{-4} | 3.658×10^{-6} | 1.741×10^{-6} | 8.812×10^{-6} | 2.189×10^{-5} |
| | R^2 | 0.999 | 0.993 | 0.992 | 0.986 | 0.991 |
| | Δq_e (%) | 35.21 | 59.62 | 74.03 | 46.38 | 27.77 |
| Banham adsorption rate equation | k (min ⁻¹) | 0.0065 | 0.0024 | 0.0271 | 0.0038 | 0.0181 |
| | z | 0.8476 | 1.3163 | 1.3393 | 1.3083 | 0.9740 |
| | q_e (mg g ⁻¹) | 307.6611 | 408.3539 | 468.6380 | 500.4855 | 491.4522 |
| | R^2 | 0.999 | 0.998 | 0.997 | 0.997 | 0.992 |
| Elovich kinetic equation | Δq_e (%) | 5.81 | 4.64 | 5.32 | 6.61 | 3.49 |
| | α_E (mg g ⁻¹ min ⁻¹) | 0.0068 | 3.884×10^{-4} | 4.405×10^{-4} | 4.922×10^{-4} | 9.919×10^{-4} |
| | β_E (g mg ⁻¹) | 0.0116 | 0.0067 | 0.0526 | 0.0056 | 0.0069 |
| | R^2 | 0.989 | 0.976 | 0.964 | 0.975 | 0.981 |

3.4 Kinetics Model Fitting Studies

Four kinetic model fitting were carried out in order to further study the adsorption dynamic processes of the VOCs by the CAC. Figure 7 shows the nonlinear fitting results of pseudo-first-order kinetic model, pseudo-second-order kinetic model, Banham adsorption rate equation model, and Elovich kinetic equation model. The values of adsorption parameters, the maximum adsorption capacity (q_e), and the correlation coefficient (R^2) are listed in Table 6.

Among the pseudo-first-order, pseudo-second-order, and Banham adsorption rate equation kinetic models, Banham model has the best fitting for all the VOCs. In general, this model is usually used to reveal the adsorption phenomenon occurred on the solid–gas interface. The best fitting by Banham model is mainly owing to the high R^2 values (above 0.99) and the smallest differences between the predicted and experimental maximum uptakes of the VOCs. Moreover, the Elovich kinetic model developed by Zeldowitsch also well fits the experimental data, owing to the high R^2 values (above 0.96). The model assumes that the surface of the solid adsorbent is energetically heterogeneous, and there is no interaction among the adsorbed species. In other words, this model mainly describes a complex heterogeneous diffusion process on the surface of the adsorbent. Additionally, as shown in Table 6, all the values of β_E were higher than those of α_E . These findings indicated that the desorption rates of all the VOCs were higher than their adsorption rates. The reason is likely that the desorption process is completed during the heating procedure (Shah et al. 2014).

4 Conclusion

In this study, the dynamic adsorption behaviors of five typical VOCs were studied by using various model fittings. Through evaluation of the maximum adsorption capacities, we found that the higher molecular weights of the VOCs had better uptakes by the selected CAC in the fixed bed system. Two dynamic adsorption models were used to describe the breakthrough curves of the VOCs. Compared to the Yoon-Nelson model, Boltzmann model has a better fitting for the experimental data, which demonstrated that the less mass transfer resistances of the VOCs had higher utilization efficiencies of the fixed bed. Among the four kinetic models,

Banham adsorption rate equation model had the best fitting result. Thus, this model can help us to more accurately evaluate the maximum uptake of the fixed adsorbent. We believe that this work is beneficial to optimize the design of dynamic adsorption system for the removal of VOCs.

References

- Aygün, A., Yenisoý-Karakaş, S., & Duman, I. (2003). Production of granular activated carbon from fruit stones and nutshells and evaluation of their physical, chemical and adsorption properties. *Microporous and Mesoporous Materials*, 66, 189–195.
- Basta, A. H., Fierro, V., El-Saied, H., & Celzard, A. (2009). 2-Steps KOH activation of rice straw: an efficient method for preparing high-performance activated carbons. *Bioresource Technology*, 100, 3941–3947.
- Biesheuvel, P., Van Limpt, B., & Van der Wal, A. (2009). Dynamic adsorption/desorption process model for capacitive deionization. *The Journal of Physical Chemistry C*, 113, 5636–5640.
- Celebioglu, A., Sen, H. S., Durgun, E., & Uyar, T. (2016). Molecular entrapment of volatile organic compounds (VOCs) by electrospun cyclodextrin nanofibers. *Chemosphere*, 144, 736–744.
- Chiang, H.-L., Chiang, P. C., & Huang, C. P. (2002). Ozonation of activated carbon and its effects on the adsorption of VOCs exemplified by methylethylketone and benzene. *Chemosphere*, 47, 267–275.
- Chuang, C. L., Chiang, P. C., & Chang, E. E. (2003). Modeling VOCs adsorption onto activated carbon. *Chemosphere*, 53, 17–27.
- Das, D., Gaur, V., & Verma, N. (2004). Removal of volatile organic compound by activated carbon fiber. *Carbon*, 42, 2949–2962.
- Dobre, T., Părvulescu, O. C., Iavorschi, G., Stroescu, M., & Stoica, A. (2014). Volatile organic compounds removal from gas streams by adsorption onto activated carbon. *Industrial & Engineering Chemistry Research*, 53, 3622–3628.
- Dumont, E., Darracq, G., Couvert, A., Couriol, C., Amrane, A., Thomas, D., Andrès, Y., & Le Cloirec, P. (2011). VOC absorption in a countercurrent packed-bed column using water/silicone oil mixtures: influence of silicone oil volume fraction. *Chemical Engineering Journal*, 168, 241–248.
- Ebner, A. D., Reynolds, S. P., & Ritter, J. A. (2006). Understanding the adsorption and desorption behavior of CO₂ on a K-promoted hydrotalcite-like compound (HTlc) through nonequilibrium dynamic isotherms. *Industrial & Engineering Chemistry Research*, 45, 6387–6392.
- Gil, R. R., Ruiz, B., Lozano, M. S., Martín, M. J., & Fuente, E. (2014). VOCs removal by adsorption onto activated carbons from biocollagenic wastes of vegetable tanning. *Chemical Engineering Journal*, 245, 80–88.
- Giraudet, S., Boulinguez, B., & Le Cloirec, P. (2014). Adsorption and electrothermal desorption of volatile organic compounds and siloxanes onto an activated carbon fiber cloth for biogas purification. *Energy & Fuels*, 28, 3924–3932.

- Guieysse, B., Hort, C., Platel, V., Munoz, R., Ondarts, M., & Revah, S. (2008). Biological treatment of indoor air for VOC removal: potential and challenges. *Biotechnology Advances*, 26, 398–410.
- Guo, Y., Li, Y., Wang, J., Zhu, T., & Ye, M. (2014). Effects of activated carbon properties on chlorobenzene adsorption and adsorption product analysis. *Chemical Engineering Journal*, 236, 506–512.
- He, X., Sun, H., Zhu, M., Yaseen, M., Liao, D., Cui, X., Guan, H., Tong, Z., & Zhao, Z. (2017). N-doped porous graphitic carbon with multi-flaky shell hollow structure prepared using a green and 'useful' template of CaCO₃ for VOC fast adsorption and small peptide enrichment. *Chemical Communications (Cambridge, England)*, 53, 3442–3445.
- Huang, Z.-H., Kang, F., Zheng, Y.-P., Yang, J.-B., & Liang, K.-M. (2002). Adsorption of trace polar methy-ethyl-ketone and non-polar benzene vapors on viscose rayon-based activated carbon fibers. *Carbon*, 40, 1363–1367.
- Hudec, P., Smiešková, A., Idek, Z., Schneider, P., & Šolcová, O. (2002). Determination of microporous structure of zeolites by t-plot method—state-of-the-art. *Studies in Surface Science and Catalysis*, 142, 1587–1594.
- López-Fonseca, R., Gutiérrez-Ortiz, J. I., & González-Velasco, J. R. (2004). Catalytic combustion of chlorinated hydrocarbons over H-BETA and PdO/H-BETA zeolite catalysts. *Applied Catalysis A: General*, 271, 39–46.
- Landers, J., Gor, G. Y., & Neimark, A. V. (2013). Density functional theory methods for characterization of porous materials. *Colloids and Surfaces A: Physicochemical and Engineering Aspects*, 437, 3–32.
- Mohan, N., Kannan, G. K., Upendra, S., Subha, R., & Kumar, N. S. (2009). Breakthrough of toluene vapours in granular activated carbon filled packed bed reactor. *Journal of Hazardous Materials*, 168, 777–781.
- Price, D. W., & Schmidt, P. S. (1998). VOC recovery through microwave regeneration of adsorbents: process design studies. *Journal of the Air & Waste Management Association*, 48, 1135–1145.
- Qian, X., Yue, D., Tian, Z., Reng, M., Zhu, Y., Kan, M., Zhang, T., & Zhao, Y. (2016). Carbon quantum dots decorated Bi₂WO₆ nanocomposite with enhanced photocatalytic oxidation activity for VOCs. *Applied Catalysis B: Environmental*, 193, 16–21.
- Shah, I. K., Pre, P., & Alappat, B. (2014). Effect of thermal regeneration of spent activated carbon on volatile organic compound adsorption performances. *Journal of the Taiwan Institute of Chemical Engineers*, 45, 1733–1738.
- Shroder, R., Nemanich, R., & Glass, J. (1990). Analysis of the composite structures in diamond thin films by Raman spectroscopy. *Physical Review B*, 41, 3738.
- Stolwijk, J. A. (1990). Assessment of population exposure and carcinogenic risk posed by volatile organic compounds in indoor air. *Risk Analysis*, 10, 49–57.
- Tefera, D. T., Hashisho, Z., Philips, J. H., Anderson, J. E., & Nichols, M. (2014). Modeling competitive adsorption of mixtures of volatile organic compounds in a fixed-bed of beaded activated carbon. *Environmental Science & Technology*, 48, 5108–5117.
- Volkamer, R., Jimenez, J. L., San Martini, F., Dzepina, K., Zhang, Q., Salcedo, D., Molina, L. T., Worsnop, D. R., & Molina, M. J. (2006). Secondary organic aerosol formation from anthropogenic air pollution: rapid and higher than expected. *Geophysical Research Letters*, 33, L17811.
- Xijun, H., Qiao, S., Zhao, X. S., & Gao Qing, L. (2001). Adsorption study of benzene in ink-bottle-like MCM-41. *Industrial & Engineering Chemistry Research*, 40, 862–867.
- Zaitan, H., Manero, M. H., & Valdes, H. (2016). Application of high silica zeolite ZSM-5 in a hybrid treatment process based on sequential adsorption and ozonation for VOCs elimination. *Journal of Environmental Sciences (China)*, 41, 59–68.
- Franz, M., Arafat, H. A., & Pinto, N. G. (2000). Effect of chemical surface heterogeneity on the adsorption mechanism of dissolved aromatics on activated carbon. *Carbon*, 38, 1807–1819.
- Wood, G. O. (2002). Quantification and application of skew of breakthrough curves for gases and vapors eluting from activated carbon beds. *Carbon*, 40, 1883–1890.
- Fuertes, A. B., & Centeno, T. A. (1998). Preparation of supported asymmetric carbon molecular sieve membranes. *Journal of Membrane Science*, 144, 105–111.
- Fujita, H., Kishimoto, A., & Matsumoto, K. (1960). Concentration and temperature dependence of diffusion coefficients for systems polymethyl acrylate and n-alkyl acetates. *Transactions of the Faraday Society*, 56, 424–437.
- Gales, L., Mendes, A., & Costa, C. (2000). Hysteresis in the cyclic adsorption of acetone, ethanol and ethyl acetate on activated carbon. *Carbon*, 38, 1083–1088.
- Huang, Y. S., & Sundmacher, K. (2007). Kinetics study of propyl acetate synthesis reaction catalyzed by Amberlyst 15. *International Journal of Chemical Kinetics*, 39, 245–253.